A combinatorial optimization design method applied to S-shaped compressor transition duct design

Hanan Lu, Xinqian Zheng and Qiushi Li

Proceedings of the Institution of Mechanical Engineers, Part G: Journal of Aerospace Engineering 2014 228: 1749
originally published online 23 April 2014
DOI: 10.1177/0954410014531922

Original Article

Institution of MECHANICAL ENGINEERS
Journal of AEROSPACE ENGINEERING

Proc IMechE Part G:
J Aerospace Engineering
2014, Vol. 228(10) 1749–1758

DOI: 10.1177/0954410014531922
uk.sagepub.com/jaero
SAGE

A combinatorial optimization design method applied to S-shaped compressor transition duct design

Hanan Lu[1], Xinqian Zheng[2] and Qiushi Li[1]

Abstract

This paper presents a combinatorial optimization method based on uniform design in combination with response surface methodology and genetic algorithm. Uniform design is used to obtain experimental points and response surface methodology to establish a mathematical regression model. Subsequently, genetic algorithm is employed to acquire optimal solution of the objective function. The optimization method has been applied to a two-dimensional S-shaped transition duct design. The process is performed with two design variables. One defines the drop height ratio which describes wall profile, and the other depicts the length ratio between the axial length of the S-shaped transition duct and the duct inlet height. Total pressure loss coefficient as an aerodynamic performance parameter is selected as the objective function for optimization. The objective function is numerically assessed at design points sampled by uniform design in the experimental domain. The initial transition duct was designed with a radius-change to length ratio 11.6% larger than current engine design limits, and the optimization yields a decrease of 36.9% in total pressure loss and more uniform distributions of parameters at the outlet. The paper shows that the described optimization method can be applied to turbofan engines to increase the radial offset and decrease the axial design space between the fans and cores without jeopardizing performance.

Keywords

Uniform design, response surface methodology, genetic algorithm, S-shaped transition duct, optimization design

Date received: 30 November 2013; accepted: 24 March 2014

Introduction

The demand for high efficiency and low fuel consumption has led to the development of turbofan engines with high bypass ratios, featuring large fans and small high pressure ratio cores. The trend towards increased radial offset and decreased axial distance between the fans and cores has drawn attention to the design of the S-shaped compressor transition duct.

An experimental investigation was undertaken by Bailey et al.[1,2] to determine the aerodynamic performance of an annular S-shaped duct. They concluded that the loss generation within the duct depends on both the pressure gradients and curvatures. Ortiz Dueñas et al.[3] described the effect of length on duct performance. These investigations have provided a large quantity of experimental data for S-shaped transition duct design. Further to the above investigations, Que et al.[4] put forward an S-shaped compressor transition duct design method based on wall pressure gradient control.

With rapid development of computer facilities and computational fluid dynamics (CFD) techniques, the process of numerical optimization has been widely applied.[5,6] Ghisu et al.[7] used CFD for performance evaluation and the steepest descent algorithm in seeking the best design to optimize an axial compressor intermediate duct through 11 geometrical variables. The achieved reduction in total pressure loss is 12.5%. Gao et al.[8] explored compressor intermediate duct design and employed a single-objective genetic algorithm (GA) combined with aerodynamic evaluation method to optimize a compressor intermediate duct. Wallin et al.[9] used four independent variables to parameterize the geometry of transition ducts and employed a face-centered composite design method combined with response surface methodology (RSM) to perform the optimization of a transition duct, and they achieved a total pressure loss reduction

[1]National Key Laboratory on Aero-engines, School of Energy and Power Engineering, Beihang University, Beijing, China
[2]State Key Laboratory of Automotive Safety and Energy, Tsinghua University, Beijing, China

Corresponding author:
Qiushi Li, National Key Laboratory on Aero-engines, School of Energy and Power Engineering, Beihang University, Beijing, China.
Email: liqs@buaa.edu.cn

of about 24%. But the number of candidate designs increases rapidly with the number of design variables in a face-centered composite design method.

In the presently established process for optimizing S-shaped transition ducts, there are two significant barriers: high computation consumption and considerable geometrical variables. In the condition of the same number of variables, compared with other experimental design methods, uniform design (UD) is adopted in this paper as it can reduce the number of candidate designs and the design time, decreasing the computation consumption. In order to avoid the complex description of wall profiles and decrease the number of geometrical variables, the midway offset ratio is introduced. Moreover, an improvement is also made in traditional RSM and a cubic regression equation is introduced to give a more accurate mathematical model which can give an accurate approximation of the relationship between the design variables and the objective.

In the present work, the optimization process is seeded with an initial duct design. As the first step, the experimental points are determined using uniform design. Then the numerical computations are introduced to acquire experimental data. And an objective function is established by using improved RSM. Finally, GA[10–12] is employed to seek the optimal solution of the objective function, while satisfying particular constraints to obtain the optimal design. Comparisons of the flow field characteristics have been made between the optimized design and the initial design.

Methodology

The optimization method is based on the combination of uniform design, response surface methodology and GA. The overall process is shown in Figure 1. Firstly, the variables of the optimization problem should be defined. Total pressure loss coefficient as an aerodynamic performance parameter is selected as the objective or the response in design of experiments (DOE). Then the parameters influencing the response should be determined. They are the independent variables or called factors in DOE. Secondly, the variation range of variables which is called the experimental domain should be also defined. In order to set up the whole process of optimization, the distributions of the experimental points in experimental domain are determined by using an appropriate uniform design table, so the experimental scheme is obtained. Thirdly, numerical calculations are employed to assess the responses of the experimental points in the experimental domain so as to obtain experimental data. Fourthly, RSM is introduced to establish a mathematical regression model based on the experimental data. Finally, GA is used to seek the optimal design point based on the mathematical model in the entire experimental domain.

Design of experiment

Based on quasi-Monte Carlo method, uniform design was established by Fang et al.[13–15] as an efficient method of experimental design. It applies commonly to experiments with many factors and many levels,[16–18] especially for the problems of mathematical model uncertain before experimental design.

Uniform design offers a lot of experimental tables. These tables give a detail description of experimental scheme. For example, a uniform design table can be depicted as $U_n(q^s)$, where U stands for uniform design, n for number of experimental trials, q for number of

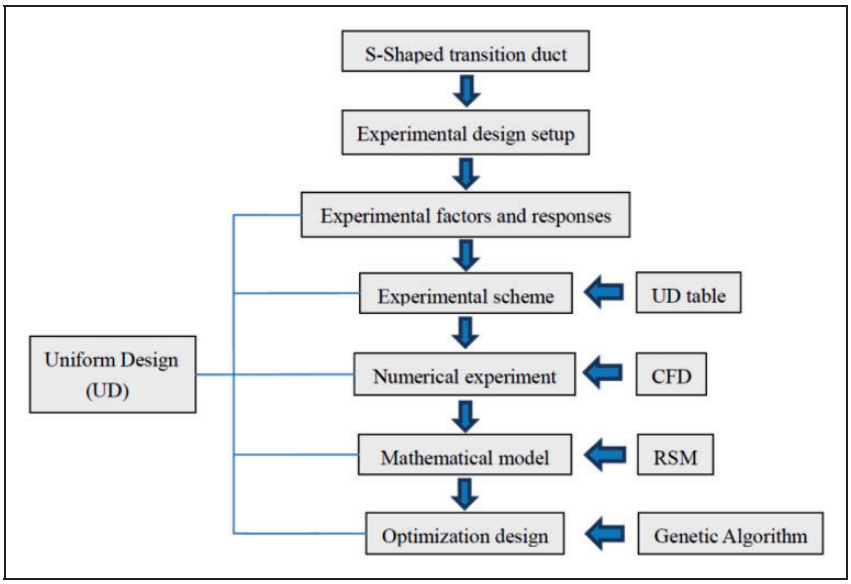

Figure 1. Flowchart of optimization.
CFD: computational fluid dynamics; RSM: response surface methodology.

levels and s for number of factors. The procedure of uniform design is described as follows:

I Choose experimental factors and domain according to the purpose of the experiment and determine a suitable number of levels for each factor.
II Select an appropriate uniform design table according to the number of factors and levels to arrange an experiment.
III Set up numerical calculations to obtain responses.
IV Establish an appropriate mathematical model.
V Seek optimal solution of the mathematical model.

Response surface methodology

Response surface methodology was developed by Box and his collaborators in the 1950s.[19] It is based on the use of a second-order equation and this method has been widely applied to aerodynamic configuration design.[20–23] Some researchers have also used RSM in combination with experimental design methods for aerodynamic design.[24,25]

A mathematical regression model approximating the objective function is constructed from the responses by using RSM. Since a traditional second-order response surface does not provide the satisfactory approximation expected, an improvement is made in traditional RSM to acquire a more accurate mathematical model. In the present work, a third-order polynomial equation is used to approximate the objective function. The response surface model takes the form of equation (1)

$$y = \beta_0 + \sum_{i=0}^{1} \beta_{1+i}\, x^{1-i}\, t^i + \sum_{i=0}^{2} \beta_{3+i}\, x^{2-i}\, t^i + \sum_{i=0}^{3} \beta_{6+i}\, x^{3-i}\, t^i + \varepsilon \quad (1)$$

where β_0 is the constant term, β_i represents the coefficients of the nonlinear parameters and the interaction parameters, while x and t represent the variables and ε is the residual associated to the experiment.

The above mathematical model is solved by using the method of least squares (MLS). In MLS, it is assumed that random errors are identically distributed with a zero mean and a common unknown variance and they are independent of each other. The difference between the observed and the fitted value $\hat{y}$ for the ith observation $\varepsilon_i = y_i - \hat{y}_i$ is called the residual and is an estimate of the corresponding ε_i. The criterion for choosing the β_j estimates is that they should minimize the sum of the squares of residuals, which is often called the sum of squares of the errors and denoted by SSE

$$SSE = \sum_{i=1}^{n} \varepsilon_i^2 = \sum_{i=1}^{n} (y_i - \hat{y}_i)^2 \quad (2)$$

The residuals can be written as

$$\varepsilon = y - X\tilde{\beta} \quad (3)$$

and the SSE is

$$SSE = \varepsilon^T \varepsilon = (y - X\tilde{\beta})^T (y - X\tilde{\beta}) \quad (4)$$

Differentiating the SSE with respect to $\tilde{\beta}$, a vector of partial derivatives can be obtained as follows

$$\frac{\partial}{\partial \tilde{\beta}}(SSE) = -2X^T (y - X\tilde{\beta}) \quad (5)$$

Equating this derivative to zero and the following equation can be obtained

$$X^T X\tilde{\beta} = X^T y \quad (6)$$

The formal solution of $\tilde{\beta}$ is then

$$\tilde{\beta} = (X^T X)^{-1} X^T y \quad (7)$$

As a measure of the quality of the response surface fit, the coefficient of determination (R^2) is introduced. It is defined by the following equation (8)

$$R^2 = \frac{SSR}{SST} = 1 - \frac{SSE}{SST} \quad (8)$$

where SSR is known as the regression sum of squares and SST as the total sum of squares. SST is defined by equation (9) as follows

$$SST = \sum_{i=1}^{n} (y_i - \bar{y})^2 \quad (9)$$

Here y_i is the calculated response of the ith design, $\hat{y}_i$ is the response surface approximation to y_i and $\bar{y}$ is the mean value of all calculated responses.

Once the response surface approximation of the objective function is constructed, seeking its optimum is a simple procedure. In the present work, GA is adopted to solve the optimization problem.

Optimal solution

GA is employed to solve the problem in this study because it is an effective method for nonlinear optimization problems. Figure 2 shows the flowchart of GA.

To set up GA, the initial size of population is selected to be 30. The crossover probability and the

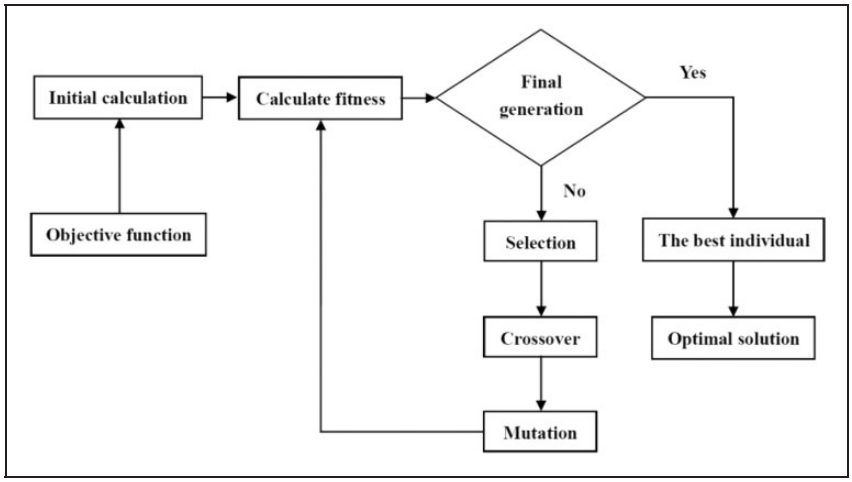

Figure 2. Flowchart of genetic algorithm.

mutation probability are selected to be 0.8 and 0.02, respectively. As to the stopping criteria, the maximum number of generation is set to be 100. The values of these parameters are selected based on the previous work. At each iteration, GA performs a series of computations on the current generation to produce a new generation. The optimal solution will be obtained at the end of the iterations.

Geometry of transition duct

Annular ducts can be found in aero-engine compressors as inter-stage components, which transmit the flow from a high radius component to a low radius component. Figure 3 shows the large annular S-shaped ducts used to connect the low- and high-pressure systems of a modern two-spool aero-engine. The drive to improve aero-engine performance requires shorter engines with higher bypass ratios. These requirements dictate S-shaped transition ducts that are shorter in length with higher radius change.

In this paper, circumferential asymmetry of inflow in the transition duct is not considered. Since the annular S-shaped duct is axial and circumferential symmetric, the optimization is undertaken on a cascade of a sector of an annular S-shaped duct. Figure 4 shows the schematic of a two-dimensional (2D) S-shaped compressor transition duct. The nondimensional design space of S-shaped ducts depends on four main parameters.[26] The four parameters that are most commonly used are $\Delta R/L$, h_{in}/L, A_{out}/A_{in}, and R_{in}/h_{in}, where ΔR stands for radial offset, L for S-shaped duct length, h_{in} for inlet height, A_{in} for inlet area, A_{out} for outlet area and R_{in} for inner wall radius at the inlet. Increasing the first three parameters by either increasing the radial offset, ΔR, or reducing the duct length, L, or increasing the outlet area, has a similar effect on the duct's performance. The large deceleration on the hub wall increases in magnitude and the flow begins to separate.

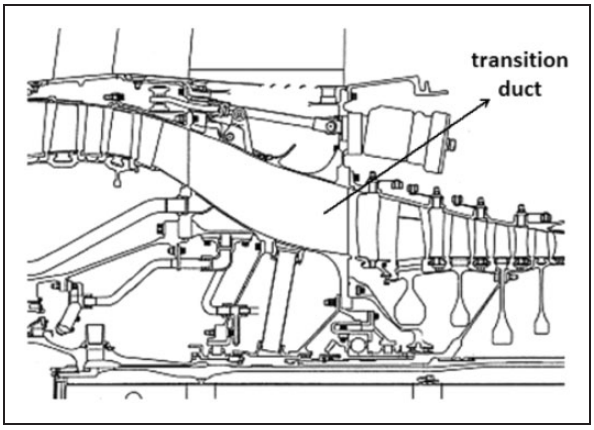

Figure 3. The compressor transition duct of a high bypass ratio aeroengine.

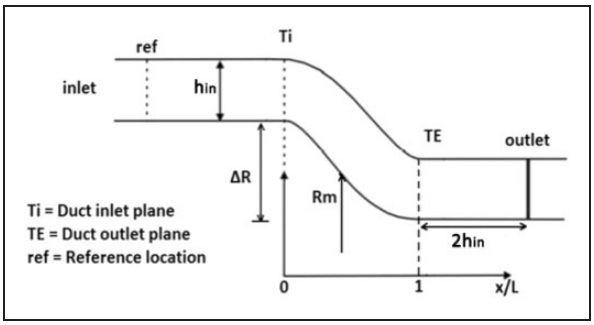

Figure 4. Schematic diagram of a 2D S-shaped transition duct.

The duct investigated in this work has an inlet to outlet area ratio of unity. A nondimensional length L/h_{in} and the midway offset ratio[4] of inner wall are together used to describe the duct geometry. The midway offset ratio ξ is defined as

$$\xi = (R_{in} - R_m)/(R_{in} - R_{out}) \tag{10}$$

where R_{out} is the radius of inner wall at outlet and R_m is the radius of inner wall at $0.5L$.

Two coefficients are introduced to assess the performance of the ducts, which are the wall static pressure coefficient and the total pressure loss coefficient, respectively. The wall static pressure coefficient is defined as

$$C_p = (P_s - P_{sref})/(P^*_{in} - P_{sref}) \quad (11)$$

where P_s is the static pressure of the investigating points on the inner wall, P^*_{in} is the stagnation pressure at the inlet of computational domain and P_{sref} is the static pressure at reference location. The reference location is shown in Figure 4.

The total pressure loss coefficient is defined as

$$\omega = (P^*_{in} - P^*_{out})/(0.5\rho U^2) \quad (12)$$

where P^*_{out} is the stagnation pressure at the outlet of computational domain, ρ is the density of fluid and U is the mean velocity at the inlet of computational domain.

Experimental design setup

In experimental design, there are two types of variable: responses and factors. In general, responses are the dependent variables and factors the independent ones. To set up an experiment, responses and factors must be determined first.

The two coefficients, the nondimensional length and the midway offset ratio of inner wall mentioned above, are selected to be the experimental factors. The total pressure loss coefficient is regarded as the response and the objective function for optimization.

Uniform design is introduced to arrange the factors to give out experimental sampling points. The criteria of uniform design is that the number of levels is no less than twice the number of factors. Based on the criteria and the number of coefficients of the nonlinear parameters in mathematical regression model, the uniform design table $U_{12}(6^2)$ is employed to arrange the experiment and the final concrete scheme of the experiment is shown in Table 1.

In the present work, there are totally two factors and either of the factors has 6 levels which are numbered 1–6. The column 2 and column 3 depict the uniform design table $U_{12}(6^2)$. The column 4 and 5 depict the magnitudes corresponding to each level of the two factors. These two columns describe the experimental sampling points of which the experimental scheme is made up.

Computational methods

The numerical investigation adopted to assess the performance of the system is performed by using commercial code ANSYS-Fluent 14.0. The solutions are obtained by solving the 2D steady compressible Reynolds-averaged Navier–Stokes equations through a finite-volume solver with a second-order upwind discretization scheme. The implicit formulations are solved. In this investigation, the Spalart–Allmaras turbulence model is used.

The computational domain is depicted in Figure 5. The inlet and outlet of the computational domain are suited two inlet heights upstream and downstream of the duct. The inlet absolute total pressure and total temperature are given along with the inlet flow angle. Average static pressure is specified at the exit. Mass average has been adopted to obtain the profile of flow parameters at the outlet of the duct. The solid surfaces in the computational domain are assumed to be adiabatic and no slip. The identical boundary conditions are used in all calculations.

An unstructured grid system is applied with a quadrilateral grid. Figure 5 also shows the computational grids of the duct. The duct profile creation and computational grid are accomplished by using ICEM CFD 14.0. Furthermore, the grid is clustered near the wall in order to obtain the detailed flowing message. The cell-centers adjacent to the walls are located at $y^+ \approx 30$ for the calculations.

For all the cases in this paper, the residual values of the continuity equation are set to fall below 1.0×10^{-6}, and the residual values of x-velocity, y-velocity, and energy equations are kept below 1.0×10^{-7}. All the cases are converged to residual levels of the order of 10^{-6}. Solutions tended to converge after approximately 5000 iterations when the mass flow error between the inlet and outlet of the computational domain is less than 1×10^{-6}. The computations are performed on a PC of 32-bit operating

Table 1. Uniform design table $U_{12}(6^2)$ and experimental scheme.

	Uniform design table $U_{12}(6^2)$		Factor levels	
Candidate design	Factor 1 (midway offset ratio ξ)	Factor 2 (nondimensional length, L/h_{in})	Value of ξ	Value of L/h_{in}
1	1	1	0.49	2.1
2	1	5	0.49	2.7
3	2	3	0.52	2.4
4	2	6	0.52	2.85
5	3	2	0.55	2.25
6	3	4	0.55	2.55
7	4	2	0.58	2.25
8	4	4	0.58	2.55
9	5	3	0.61	2.4
10	5	6	0.61	2.85
11	6	1	0.64	2.1
12	6	5	0.64	2.7

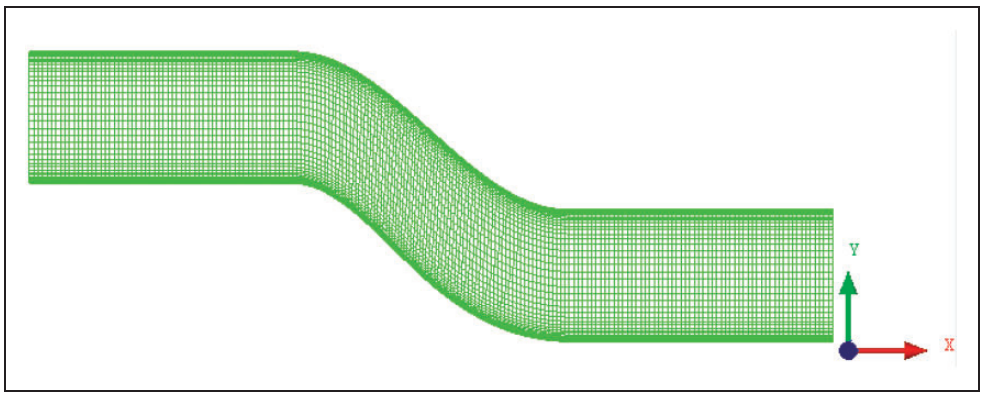

Figure 5. Grid for the 2D S-shaped duct geometry.

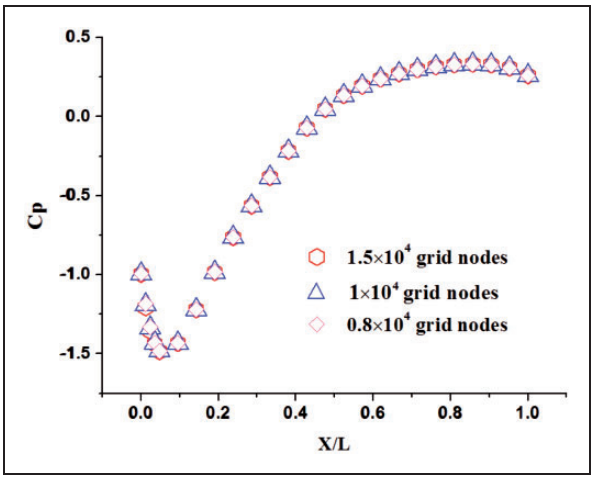

Figure 6. C_p distribution on the inner wall with different grid nodes.

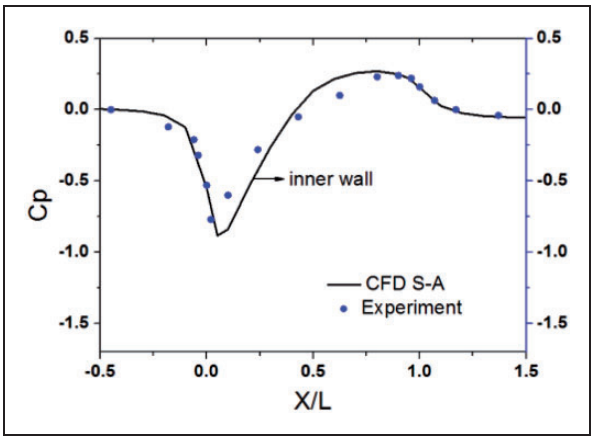

Figure 7. Comparison of the C_p distribution on the inner wall between the experimental results and numerical simulations.

system with Genuine Intel(R) CPU (4CPUs). The computational time for one case is approximately 25 min depending on the length of the duct geometry and the rate of convergence.

A grid independence check is carried out. Take one case for example, a 2D S-shaped duct is calculated with different grid densities. The number of grid nodes in both x and y directions is changed with different total number of grid nodes. The results show that the C_p distribution on the inner wall is nearly unchanged when the total number of grid nodes vary from 0.8×10^4 to 1.5×10^4 which is depicted in Figure 6. Therefore, the numerical calculation is performed with 1×10^4 grid nodes for this case. For other cases, the number of grid nodes is determined in the same method as above.

Result and discussion

Validation of numerical method

The numerical results for the C_p distribution on inner wall obtained by using the above numerical method are compared with the experimental results.[3] The duct has an area ratio of unity. The nondimensional length $h_{in}/L = 0.30$ and the radial offset $\Delta R/L = 0.5$. The comparison was conducted at the points on the inner wall and the results are shown in Figure 7. It shows good agreement between the numerical and experimental results which further illustrates that the numerical method is accurate in this study.

Assessment of mathematical model

Since the behavior of the system is unknown, it is essential to check whether the mathematical model fits well to the experimental data. For verification of the model adequacy, variance analysis is made. The coefficient of determination (R^2) and F-value are both introduced. The former represents the effect of approximation of a mathematical model while the latter depicts the appropriateness. The closer the value of R^2 is to 1.0, the better effect of approximation can be obtained. At the same time, the larger the F-value is, the better appropriateness can be acquired.

The basic thought of variance analysis is to divide the total sum of squares (SST) into regression sum of squares (SSR) and error sum of squares (SSE) as

Table 2. Variance analysis of mathematical model.

Variance	Degree of freedom	Sum of squares	Mean square	*F*-value
Regression	9	*SSR* 0.002059295	0.00022881 1	424.5
Error	2	*SSE* 0.000001078	0.000000539	–
Total	11	*SST* 0.002060373	–	–

SSR: regression sum of squares; SSE: error sum of squares; SST: total sum of squares.

depicted in section "Response surface methodology". The degree of freedom of each kind of variance can be obtained according to regression analysis methods. Mean squares can be calculated by using sum of squares divided by the corresponding degree of freedom. Finally, with the larger mean square divided by the smaller one, *F*-value can be obtained. The results are shown in Table 2.

The coefficient of determination (R^2) can be calculated as follows

$$R^2 = \frac{SSR}{SST} = \frac{0.002059295}{0.002060373} = 0.999477 \quad (13)$$

$$F = 424.5 \gg F_{0.05}(9, 2) = 19.4 \quad (14)$$

From the results of the variance analysis, R^2 is very close to 1.0 and the *F*-value is much larger than $F_{0.05}$ (9, 2). It can be seen that the model is appropriate and can give a rather perfect description of the problem.

Result of optimization

In preliminary design, the transition duct had an inlet to outlet area ratio of unity and the inlet height was 0.2 m. The nondimensional length L/h_{in} was 2.15 and another nondimensional parameter R_{in}/h_{in} was 4. The radius change to length ratio $\Delta R/L$ was 0.558 that was 11.6% larger than current engine design limits.

Initial and optimized duct geometries are depicted in Figure 8. The midway offset ratio of the optimized duct is increased and the curvature of the inner wall is changed. So a more moderate pressure gradient distribution is obtained despite the smaller nondimensional length of the duct. The optimization yields a decrease of 36.9% in total pressure loss. It means that with shorter length, total pressure loss of the duct still decreases. The geometric parameters between initial design and optimized design are also compared and the results are shown in Table 3.

Figure 9 gives a description of outlet velocity distribution of the optimized duct and the initial duct. It can be clearly observed that the optimized design has more uniform inflow contours of the axial velocity component. The size of low speed region near the endwalls in the optimized design is much smaller than that in the initial one. Or rather, the boundary layer near the wall is much thinner. The wall

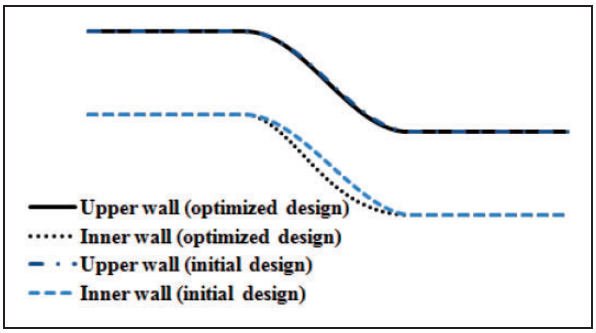

Figure 8. Comparison of initial and optimized duct geometries.

Table 3. Comparison of geometric parameters between initial and optimized designs.

	Nondimensional length, L/h_{in}	Midway offset ratio, ξ	Total pressure loss coefficient
Initial design	2.15	0.49	0.08535
Optimized design	2.1	0.64	0.05386

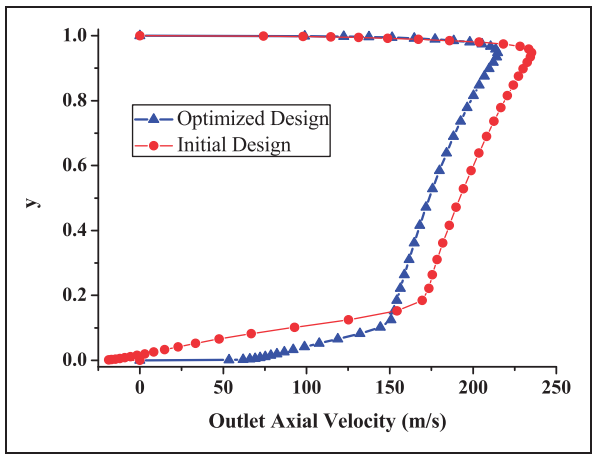

Figure 9. Comparison of the outlet velocity distribution between optimized design and initial design.

curvature of the optimized design is thought to contribute to decrease the boundary-layer separation loss.

Figure 10 depicts the comparison of outlet total pressure distribution between the optimized design and the initial design. With the same inlet total pressure, the outlet total pressure distribution of the optimized design is much more uniform than that of the initial one which illustrates that the optimized design yields lower total pressure loss than the initial one.

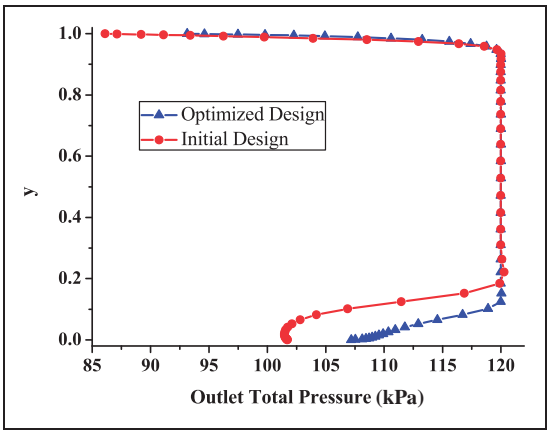

Figure 10. Comparison of the outlet total pressure distribution between optimized design and initial design.

Analysis of flow field

The purpose of flow analysis is to give a powerful physical explanation that the optimized design model yields lower losses comparing with the initial one. Figures 11 and 12 depict the distribution of static pressure in flow path of initial design and optimized design respectively. From the two figures, it can be obviously seen that the streamwise pressure gradient of initial design is much larger than that of optimized design.

By increasing the magnitude of midway offset ratio, the curvature of the inner wall is changed and the streamwise area increases. The original extent of diffusion becomes more moderate. Although the length of the optimized transition duct slightly decreases, the streamwise pressure gradient still decreases as shown in Figure 12. In Figure 13, it shows that the C_p distribution on the inner wall in optimized duct is more moderate than that in initial duct. With more appropriate C_p distribution on the inner wall, the flow is robust and not intended to separate.

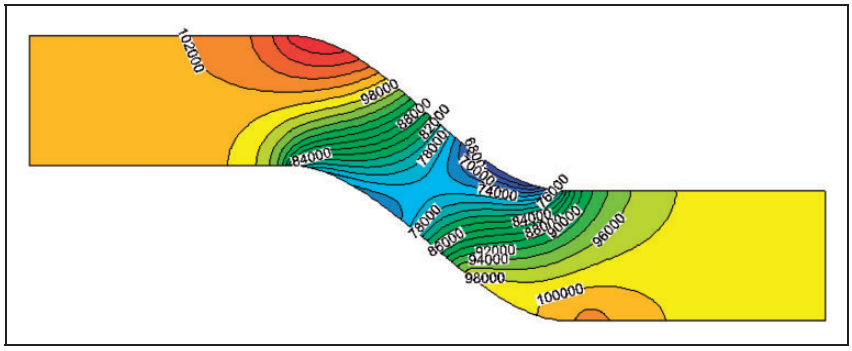

Figure 11. Distribution of static pressure in flow field of initial design.

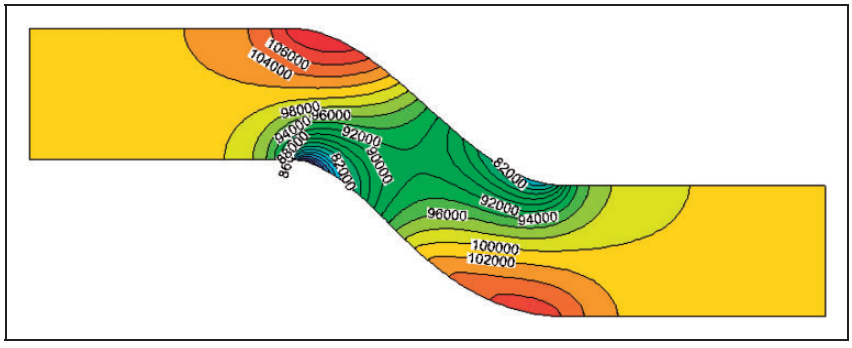

Figure 12. Distribution of static pressure in flow field of optimized design.

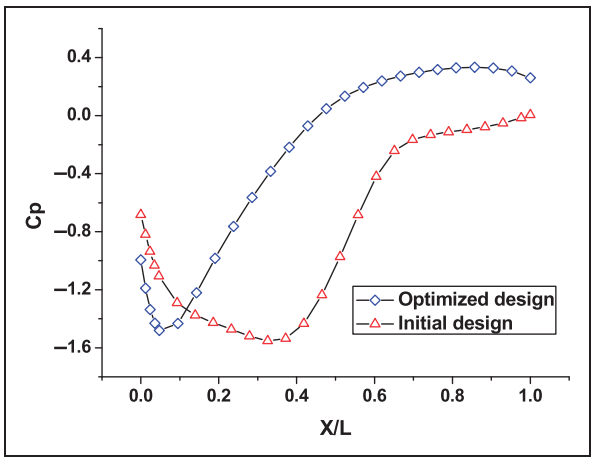

Figure 13. Comparison of the C_p distribution on inner wall between initial design and optimized design.

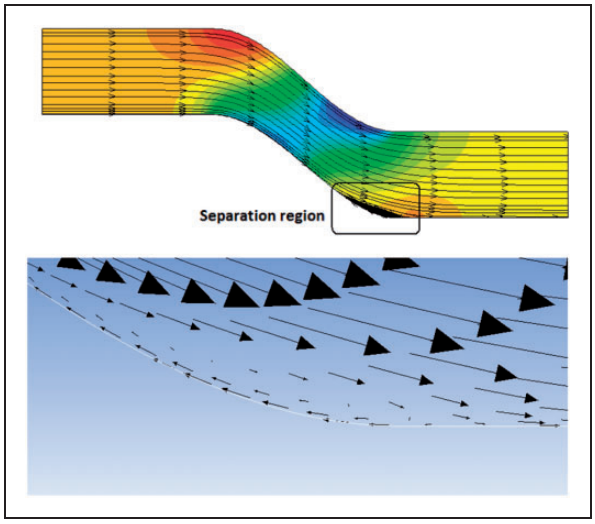

Figure 14. Streamlines in flow path of initial duct.

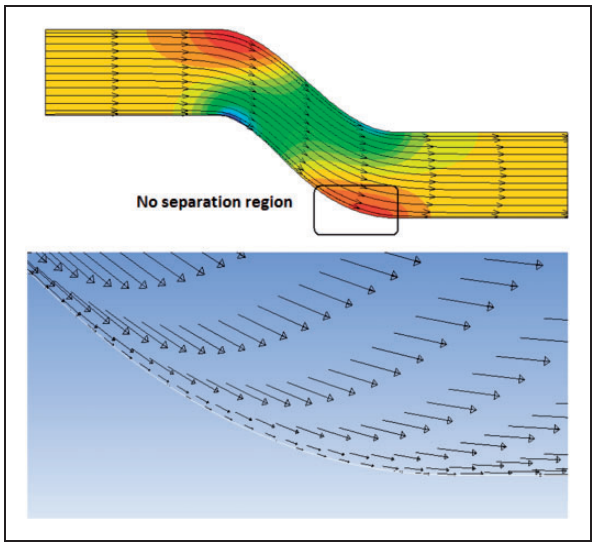

Figure 15. Streamlines in flow path of optimized duct.

Figures 14 and 15 depict the streamlines in flow path of initial duct and optimized duct respectively. It can be easily seen that there is a large boundary-layer separation region at the outlet of the S-shaped section in Figure 14. With the decrease of streamwise pressure gradient in optimized design, the boundary-layer separation region disappears as shown in Figure 15.

From the above analysis, it can be seen that the optimized design yields lower energy losses and has more uniform outlet parameters than the initial one. So the total pressure loss coefficient of the optimized design is much smaller than that of the initial one.

Conclusions

An optimization design method based on uniform experimental design in combination with response surface methodology and GA has been proposed in this paper. The successful application of the method is able to reach the optimization objective in increasing aerodynamic capability of an S-shaped transition duct. The results demonstrate the feasibility of the combinatorial optimization design method.

Moreover, as the experimental points are properly selected and uniformly distributed in the entire experimental domain, the optimization design method is capable of producing experimental points with high representativeness and these experimental points can give a full description of the system. So the method can reduce the computation consumption and design time. This further illustrates that the method is effective and has the potential to be applied to wider fields of optimization.

Funding

This research was supported by the National Natural Science Foundation of China (Grant No. 51176005).

Conflict of interest

None declared.

References

1. Bailey DW, Britchford KM, Carrotte JF, et al. Performance assessment of an annular S-shaped duct. *J Turbomach* 1997; 119(1): 149–156.
2. Bailey DW. *The aerodynamic performance of an annular S-shaped duct*. PhD Thesis, University of Loughborough, Leics, UK, 1997.
3. Ortiz Dueñas C, Miller RJ, Hodson HP, et al. Effect of length on compressor inter-stage duct performance. ASME Paper GT2007-27752, 2007.
4. Que XB, Hou AP and Zhou S. S-shaped compressor transition duct design based on wall pressure gradient control. *Acta Aeronaut Astronaut Sin* 2010; 31(3): 459–465.
5. Ellbrant L, Eriksson LE and Martensson H. Design of compressor blades considering efficiency and stability

using CFD based optimization. ASME Paper GT2012-69272, 2012.
6. Kim JH and Kim KY. Analysis and optimization of a vaned diffuser in a mixed flow pump to improve hydrodynamic performance. *J Fluids Eng* 2012; 134(7): 071104.
7. Ghisu T, Molinari M, Parks GT, et al. Axial compressor intermediate duct design and optimization. AIAA Paper 2007-1868, 2007.
8. Gao LM, Feng XD, Chen X, et al. Exploration about compressor intermediate duct design. *Acta Aeronaut Astronaut Sin* 2013; 34(5): 1057–1063.
9. Wallin F and Eriksson LE. Response surface-based transition duct shape optimization. ASME Paper GT2006-90978, 2006.
10. Gallagher K and Sambridge M. Genetic algorithms: a powerful tool for large-scale nonlinear optimization problems. *Comput Geosci* 1994; 20(7–8): 1229–1236.
11. Zhou M and Sun SD. *Genetic algorithms: Theory and applications*. Beijing: National Defence Industrial Press, 1999, pp.18–65.
12. David JC and Birk AM. Numerically optimizing an annular diffuser using a genetic algorithm with three objectives. ASME Paper GT2012-68205, 2012.
13. Fang KT, Lin DKJ, Winker P, et al. Uniform design: Theory and application. *Technometrics* 2000; 42(3): 237–248.
14. Fang KT. *Uniform design and uniform design tables*. Beijing: Science Press, 1994.
15. Fang KT, Li RZ and Sudjianto A. *Design and modeling for computer experiments*. New York: Taylor & Francis Group, LLC, 2006.
16. Wang Z and Fang KT. The uniform design with qualitative factors. *Appl Stat Manage* 1999; 18(5): 11–19.
17. Wang J, Chen BL, Rao XZ, et al. Optimization of culturing conditions of porphyridium cruentum using uniform design. *World J Microbiol Biotechnol* 2007; 23(10): 1345–1350.
18. Li WH, Liu LJ and Gong WG. Multi-objective uniform design as a SVM model selection tool for face recognition. *Expert Syst Appl* 2011; 38(6): 6689–6695.
19. Bas D and Boyac IH. Modeling and optimization I: Usability of response surface methodology. *J Food Eng* 2007; 78(3): 836–845.
20. Liu XM and Zhang WB. Two schemes of multi-objective aerodynamics optimization for centrifugal impeller using response surface model and genetic algorithm. ASME Paper GT2010-23775, 2010.
21. Luo DH. Optimization of total polysaccharide extraction from dioscorea nipponica makino using response surface methodology and uniform design. *Carbohydr Polym* 2012; 90(1): 284–288.
22. Devanathan S and Koch PN. Comparison of meta-modeling approaches for optimization. ASME Paper IMECE2011-65541, 2011.
23. Kim JH, Kim JW and Kim JY. Axial-flow ventilation fan design through multi-objective optimization to enhance aerodynamic performance. *J Fluids Eng* 2011; 133(10): 101101.
24. Wang GG. Adaptive response surface method using inherited latin hypercube design points. *J Mech Des* 2003; 125(2): 210–220.
25. Zhu CY and Qin GL. Design technology of centrifugal fan impeller based on response surface methodology. ASME Paper FEDSM-ICNMM 2010-30002, 2010.
26. Naylor EMJ, Ortiz DC, Miller RJ, et al. Optimization of nonaxisymmetric endwalls in compressor S-shaped ducts. *J Turbomach* 2008; 132(1): 011011.

Appendix

Notation

A_{in}	inlet area
A_{out}	outlet area
C_p	wall static pressure coefficient
h_{in}	duct inlet height
L	duct length
n	number of candidate designs
P^*_{in}	stagnation pressure at inlet of computational domain
P^*_{out}	stagnation pressure at outlet of computational domain
P_s	static pressure of investigating points at inner wall
R_m	radius of inner wall at $0.5L$
R_{in}	radius of inner wall at inlet
R_{out}	radius of inner wall at outlet
t	nondimensional length ratio
U	mean velocity at inlet of computational domain
x	midway offset ratio
y	objective function
y^+	nondimensional wall distance
ΔR	change in offset from inlet to outlet
ω	total pressure loss coefficient
ρ	density of fluid

Subscript

ref	reference location